β decay of ^{61,63}V and low-energy level schemes of ^{61,63}Cr

S. Suchyta,[1,2] S. N. Liddick,[1,2] C. J. Chiara,[3,4] W. B. Walters,[3] M. P. Carpenter,[4] H. L. Crawford,[5,*] G. F. Grinyer,[6] G. Gürdal,[7,†] A. Klose,[1,2,‡] E. A. McCutchan,[4,§] J. Pereira,[1] and S. Zhu[4]

[1]*National Superconducting Cyclotron Laboratory (NSCL), Michigan State University, East Lansing, Michigan 48824, USA*
[2]*Department of Chemistry, Michigan State University, East Lansing, Michigan 48824, USA*
[3]*Department of Chemistry and Biochemistry, University of Maryland, College Park, Maryland 20742, USA*
[4]*Physics Division, Argonne National Laboratory, Argonne, Illinois 60439, USA*
[5]*Nuclear Science Division, Lawrence Berkeley National Laboratory, Berkeley, California 94720, USA*
[6]*Grand Accélérateur National d'Ions Lourds (GANIL), CEA/DSM-CNRS/IN2P3, Bvd Henri Becquerel, 14076 Caen, France*
[7]*Nuclear Engineering Division, Argonne National Laboratory, Argonne, Illinois 60439, USA*

(Received 10 May 2013; revised manuscript received 21 January 2014; published 21 March 2014)

Background: Near $N = 40$, rapid development of collectivity has been inferred based on the low-energy level schemes of the even-even Fe and Cr isotopes and attributed to deformation arising primarily from the influence of the $\nu g_{9/2}$ intruder orbital. The level schemes of the odd-A Co and Fe isotopes, as well as the odd-odd Co and Mn isotopes, are also influenced by the $g_{9/2}$ orbital and suggest prolate deformation. However, scarce information is available regarding the neutron-rich odd-A Cr isotopes.

Purpose: Determine low-energy level schemes of the neutron-rich Cr isotopes approaching $N = 40$ and investigate the influence of the $\nu g_{9/2}$ orbital.

Method: Neutron-rich V isotopes were produced at the NSCL through projectile fragmentation. The β decay of the V isotopes into Cr isotopes was studied, and the observed β-delayed γ rays were used to determine the low-energy level schemes of the neutron-rich Cr isotopes.

Results: A greatly expanded level scheme is constructed for ^{61}Cr, which has an increased low-energy level density relative to isotopic ^{55,57,59}Cr. Excited states are discovered in ^{63}Cr for the first time.

Conclusion: The distinct difference between the low-energy level scheme of ^{61}Cr and the lighter neutron-rich odd-A Cr isotopes is inferred to be due to the influence of the $\nu g_{9/2}$ intruder orbital and suggests the possibility of low-energy positive-parity states in ^{61}Cr, leading to the conclusion that a significant change in deformation and orbital occupancies has taken place when N exceeds 36.

DOI: 10.1103/PhysRevC.89.034317 PACS number(s): 23.40.−s, 21.10.−k, 27.50.+e

I. INTRODUCTION

The neutron-rich nuclei near $N = 40$ have received significant attention due to the rapid development of collectivity below the Ni isotopes. As $^{68}_{28}$Ni$_{40}$ has a high-energy first excited 2^+ state [1] and a low $B(E2; 2_1{}^+ \rightarrow 0_1{}^+)$ value [2,3], a subshell gap was originally proposed at $N = 40$. However, this subshell closure is very fragile and disappears as protons are removed from ^{68}Ni. In the even-even Fe and Cr isotopes, collectivity develops as $N = 40$ is approached, inferred from the consistent decrease in the energy of the $2_1{}^+$ states [4,5] and the corresponding increase in $B(E2)$ values [6–8] along the respective isotopic chains.

The collectivity in the neutron-rich Fe and Cr isotopes has largely been attributed to the presence of prolate deformation arising from the influence of the $g_{9/2}$ and $d_{5/2}$ neutron orbitals [9,10]. As protons are removed from the $f_{7/2}$ orbital below ^{68}Ni, the attractive monopole interaction between protons in the $f_{7/2}$ orbital and neutrons in the $f_{5/2}$ orbital decreases [10]. The $\nu f_{5/2}$ orbital is pushed toward the $N = 40$ gap, increasing the probability of neutron excitations out of the fp shell [10].

In the odd-A neutron-rich nuclei near $N = 40$, the presence of prolate deformation has been inferred from the low-energy level schemes, and the importance of both proton and neutron intruder states has been suggested. In $^{67}_{27}$Co$_{40}$, an isomer was observed at 492 keV and assigned a spin and parity of $1/2^-$ due to a prolate-deformed proton intruder configuration [11]. Based on systematics, the 1095-keV state in ^{65}Co was attributed to the same proton intruder configuration [12]. Regarding neutron intruder states, in the odd-A Fe isotopes beginning at $N = 33$, states described by neutron excitations into the $g_{9/2}$ orbital have been identified, with the energy of these states decreasing as N increases. The excitation energy of the $9/2^+$ state is 1517 keV in ^{59}Fe [13] and falls to 394 keV in ^{65}Fe [14]. A positive parity state has also tentatively been identified around 400 keV in ^{67}Fe [15].

In the odd-odd Co and Mn nuclei, evidence for the coupling of intruder proton and neutron states has been obtained. Similarities have been suggested between the low-energy level schemes of the $^{66,68}_{27}$Co$_{39,41}$ and $^{64,66}_{25}$Mn$_{39,41}$ nuclei. The ground states in ^{64,66}Mn and ^{66}Co, as well as the 1.6-s isomeric state in ^{68}Co, were proposed to be prolate deformed and assigned as 1^+ based on the deformed coupling of the proton $[321]1/2^-$ state with the neutron $[301]1/2^-$ state at $\beta_2 \sim 0.2$ [16,17]. Furthermore, the first excited states in ^{64,66}Mn were identified

*Present Address: Department of Physics and Astronomy, Ohio University, Athens, Ohio 45701.
†Present Address: Physics Department, Millsaps College, Jackson, Mississippi 39210.
‡Present Address: National Institute of Standards and Technology, Boulder, Colorado 80305.
§Present Address: National Nuclear Data Center, Brookhaven National Laboratory, Upton, New York 11973-5000.

as 2^- based on the coupling of the same $1/2^-$ proton intruder with a neutron intruder state originating from the $g_{9/2}$ orbital [16]. Lastly, the negative-parity bandhead arising from the coupling of the $\pi f_{7/2}$ and $\nu g_{9/2}$ orbitals has been found to steadily decrease in energy in the odd-odd Mn isotopes between $N = 33$ and $N = 37$, analogous to the drop in energy of the positive-parity states originating from the $g_{9/2}$ orbital in the odd-A Fe isotopes [18].

The present study focuses on the low-energy level schemes of the odd-A $^{61,63}Cr_{37,39}$ isotopes populated through the β decay of ^{61,63}V. The experimental techniques that were used are described in Sec. II. The experimental results and decay schemes for the β decay of the V isotopes into the respective Cr isotopes are presented in Sec. III. The low-energy level schemes of the neutron-rich odd-A Cr isotopes are compared to shell-model calculations in Sec. IV, where the influence of the $g_{9/2}$ orbital is discussed. Finally, conclusions are stated in Sec. V.

II. EXPERIMENTAL DESCRIPTION

A 130-MeV/A ^{76}Ge primary beam was accelerated through the Coupled Cyclotron Facility at the National Superconducting Cyclotron Laboratory (NSCL) and impinged on a ^{9}Be target to produce the neutron-rich ^{61,63}V isotopes. The secondary ions of interest were selected using the full 5% momentum acceptance of the A1900 fragment separator [19]. The cocktail ion beam was transported to the Beta Counting System (BCS) [20] and implanted into a 1-mm-thick Si double-sided strip detector (DSSD) with 40 1-mm strips on the front and 40 perpendicular 1-mm strips on the back. The ions delivered to the experimental end station were characterized on an event-by-event basis using energy-loss and time-of-flight techniques. The energy loss of the ions was measured in a Si PIN detector located upstream relative to the DSSD. Time-of-flight was measured between a position-sensitive scintillator at the A1900 intermediate dispersive image and the PIN detector. The particle identification plot of the ions that were implanted into the DSSD is shown in Fig. 1. β-decay electrons were detected by the DSSD and correlated in software with preceding implanted ions based on the spatial locations of the implant and decay, as well as temporal information. The

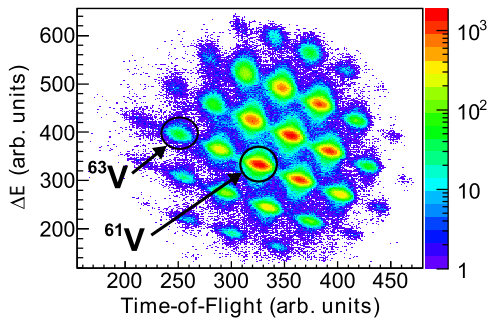

FIG. 1. (Color online) Particle identification plot for the nuclei delivered to the experimental end station characterized on an event-by-event basis using time-of-flight and ΔE methods. The β-decaying ^{61,63}V isotopes are indicated.

Segmented Ge Array (SeGA) [21], arranged in two concentric rings of eight detectors each, surrounded the BCS and was used to detect β-delayed and isomeric γ rays. The absolute efficiency of SeGA was measured as a function of energy using a calibrated source, and the total efficiency was 8.7% at 662 keV. The lower half-life limit that could be identified by measuring the time delay between coincident γ rays was approximately 150 ns.

All detector signals were independently triggered and time-stamped with a 10-ns resolution using the NSCL Digital Data Acquisition System (DDAS) [22,23]. An external validation, constructed from the AND of two OR signals, was required to record data from the DSSD. The first OR was generated following a signal above threshold in any one of the 40 strips on the front of the DSSD and the second OR was created following a signal above threshold in any one of the 40 strips on the back. In software, events were constructed by grouping together all detector signals that occurred within a 10-μs time period.

III. RESULTS

A. ^{61}Cr

The β decay of ^{61}V was used to populate low-energy states in ^{61}Cr. The β-delayed γ-ray energy spectrum within 250 ms of the arrival of a ^{61}V ion at the experimental end station is shown in Fig. 2. γ-ray transitions were identified in ^{61}Cr based on their β-gated half-lives, observed γ-γ coincidences, and previous experimental results [24]. The transitions belonging to ^{61}Cr are listed in Table I along with their absolute intensities. Sixteen transitions in ^{61}Cr were identified based on Fig. 2, and two others became apparent in coincidence spectra. The background-subtracted β-delayed γ-γ coincidence spectra gated on the three lowest-energy transitions in ^{61}Cr are shown in Fig. 3. As indicated in Fig. 3(a), the 71-keV γ ray is coincident with the three transitions at 331, 645, and 1151 keV. Eight transitions coincident with the 98-keV γ ray are apparent in Fig. 3(b), including the 408-keV transition, which is also coincident with the 127-keV γ ray based on Fig. 3(c).

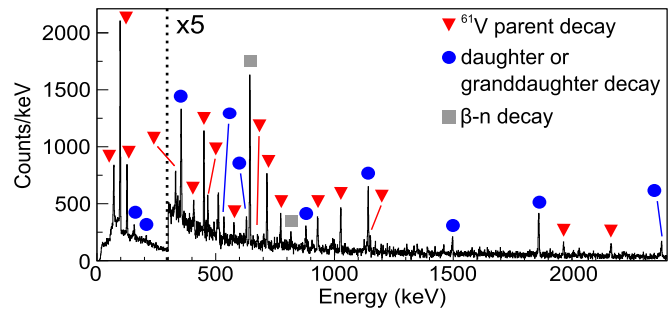

FIG. 2. (Color online) The β-delayed γ-ray energy spectrum detected within 250 ms following the implantation of a ^{61}V ion into the DSSD. Red inverted triangles mark γ rays attributed to the decay of ^{61}V, which are also listed in Table I with their respective absolute intensities. Blue circles denote γ rays attributed to daughter and granddaughter activities. Gray squares label γ rays associated with β-delayed neutron emission.

TABLE I. Energies and absolute intensities per 100 β decays for the γ-ray transitions identified in ^{61}Cr following the β decay of ^{61}V.

E (keV)	Abs. inten. (%)	E (keV)	Abs. inten. (%)
70.8(3)	9.3(8)	645.0(8)[a]	1.0(4)
97.7(3)	24.9(8)	676.4(6)	0.9(4)
126.7(3)	8.1(5)	715.9(4)	5.1(6)
331.0(4)	1.7(5)	773.7(4)	2.3(5)
353.6(5)[a]	1.2(4)	929.4(4)	3.7(5)
407.6(7)	1.7(7)	1026.3(4)	4.7(6)
450.5(3)	4.5(5)	1151.2(4)	1.4(3)
467.0(4)	1.5(4)	1964.5(4)	2.2(7)
576.7(4)[b]	0.7(3)	2164.0(5)	2.5(8)

[a]Transition observed in coincidence spectra only.
[b]Transition not placed in ^{61}Cr level scheme.

The deexcitation of the previously reported excited states at 97, 450, and 1027 keV in ^{61}Cr [24] are confirmed by the present data. Prior to this work, 71-, 127-, and 329-keV transitions were unplaced in the ^{61}Cr level scheme, but with the increased statistics, their placements are suggested. The 71-keV γ ray is proposed to directly feed the ground state based on the lack of observed coincidence with any other transition that populates the ground state. From the β-delayed γ-γ coincidence spectra, the 127-keV transition is inferred to populate the 98-keV state. The observation of several excited states which decay to both the 98-keV state and the ground state confirms the ordering of the 98- and 127-keV transitions. The 331-keV γ ray, assumed to be the same as the 329-keV transition in Ref. [24], is proposed to feed the 71-keV state based on observed γ-γ coincidence and the lower absolute intensity compared to the intensity of the 71-keV γ ray. In Ref. [24], the 717-keV transition was placed connecting the 1027-keV state with a proposed state at 310 keV. Here, the 716-keV γ-ray transition, assumed to be the same as identified at 717 keV in Ref. [24], is reassigned as directly feeding the ground state based on a lack of coincidences between it and transitions from any state at 310 keV or lower, including the 71- and 98-keV γ rays. In addition, no γ rays were observed that could be attributed to the decay of a 310-keV state. γ rays at 86, 212, or 239 keV to the 224-, 98-, or 71-keV state were not observed in the ^{61}V β-delayed γ-ray energy spectrum, nor were γ rays with these energies found in coincidence with the 127-, 98-, or 71-keV transitions. Thus, the state at 310 keV in ^{61}Cr proposed in Ref. [24] is removed.

Based on the observation of an intense 644-keV γ ray [25] in Fig. 2, a significant β-delayed neutron ($\beta - n$) emission branch is deduced for ^{61}V. An 817-keV γ ray, attributed to the $4^+ \rightarrow 2^+$ transition in ^{60}Cr [26], was found in coincidence with the 644-keV transition, confirming the β-delayed neutron emission. However, the intensity of the 817-keV transition following $\beta - n$ decay from ^{61}V is very weak and only about 0.6%. Based on the absolute intensity of the 644-keV γ ray, a lower limit of 10% is inferred for the ^{61}V $\beta - n$ branching ratio.

The β-decay curve for ^{61}V is shown in Fig. 4(a). The fit to the decay curve included contributions from the exponential

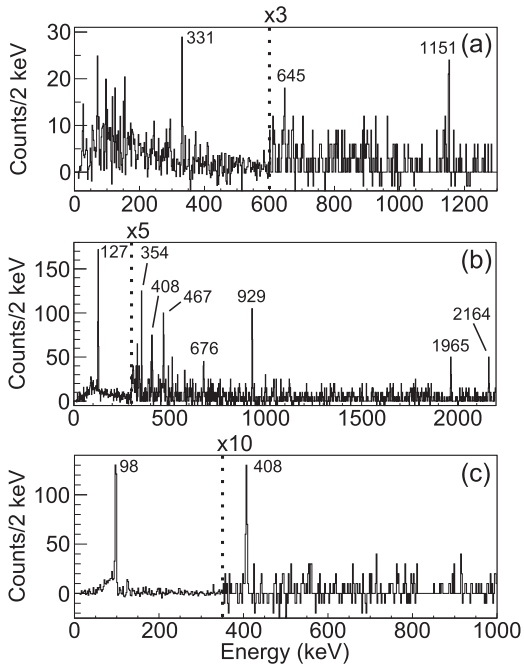

FIG. 3. Background-subtracted ^{61}V β-delayed γ-γ coincidence spectra gated on the (a) 71-keV, (b) 98-keV, and (c) 127-keV transitions.

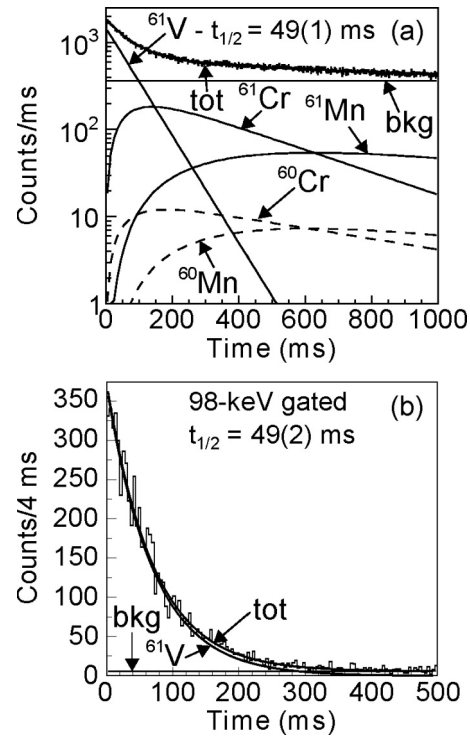

FIG. 4. (a) The β-decay curve for ^{61}V from 0 to 1 s. The overall fit, labeled "tot," includes contributions from the decay of ^{61}V, ^{61}Cr, ^{61}Mn, ^{60}Cr, and ^{60}Mn, and a constant background. The contributions from the nuclei populated through β-delayed neutron emission are shown with dashed lines. (b) The ^{61}V β-decay curve from 0 to 500 ms gated on the 98-keV transition. The curve was fit using an exponential plus a constant background.

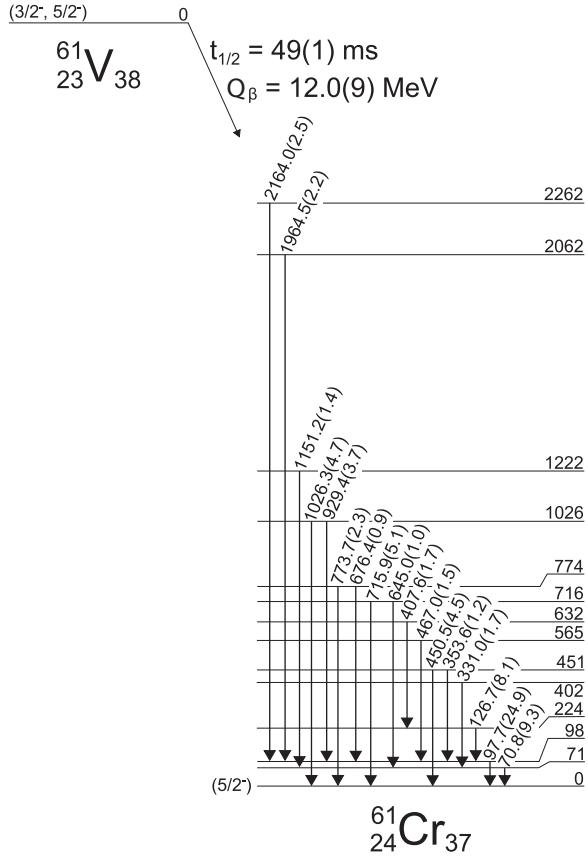

FIG. 5. Low-energy level scheme of ^{61}Cr inferred from the β decay of ^{61}V. The β-decay Q value was taken from Ref. [31]. The absolute intensity of each γ-ray transition is shown in parentheses following the transition energy.

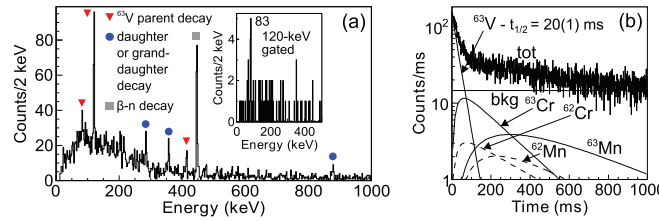

FIG. 6. (Color online) (a) The β-delayed γ-ray energy spectrum detected within 150 ms following the implantation of a ^{63}V ion into the DSSD. Red inverted triangles mark γ rays attributed to the decay of ^{63}V, which are also listed in Table II with their respective absolute intensities. Blue circles denote γ rays attributed to daughter and granddaughter activities. Gray squares label γ rays associated with β-delayed neutron emission. Inset: The β-delayed γ-γ coincidence spectrum gated on the 120-keV transition. (b) The β-decay curve for ^{63}V from 0 to 1 s. The overall fit, labeled "tot," includes contributions from the decay of ^{63}V, ^{63}Cr, ^{63}Mn, ^{62}Cr, and ^{62}Mn, and a constant background. The contributions from the nuclei populated through β-delayed neutron emission are shown with dashed lines.

decay of ^{61}V, the growth and decay of ^{61}Cr daughter, ^{61}Mn granddaughter, ^{60}Cr, and ^{60}Mn, and a constant background. The $A = 60$ nuclei were populated by $\beta - n$ decay. The half-lives of the Cr and Mn isotopes were fixed at their respective literature values: ^{61}Cr, 233 ms [27]; ^{61}Mn, 670 ms [28]; ^{60}Cr, 490 ms [29]; and ^{60}Mn, 280 ms [29]. Furthermore, the $\beta - n$ branching ratio was fixed according to the absolute intensity of the 644-keV transition. The ^{61}V half-life was determined to be 49(1) ms, in agreement with previously published results of 43(7) ms [30] and 47.0(12) ms [25]. The $\beta - n$ branching ratio had only a minor influence on the determination of the ^{61}V half-life. Increasing the branching ratio from 10% to 25% only changed the half-life by about 2 ms. For the most intense ^{61}Cr transitions in Fig. 2, γ-gated β-decay curves were constructed. The half-lives obtained by fitting the γ-gated β-decay curves to an exponential plus a constant background agreed with the half-life extracted from the ungated ^{61}V decay curve. A representative example, the 98-keV-gated ^{61}V β-decay curve, is shown in Fig. 4(b), for which a half-life of 49(2) ms was determined.

The low-energy level scheme of ^{61}Cr populated by the β decay of ^{61}V is shown in Fig. 5. The present study has revealed 13 excited states in ^{61}Cr and 9 new γ rays, greatly extending the level scheme presented in Ref. [24]. All coincidences indicated in Fig. 5 were observed. Two γ-ray transitions at 354 and 645 keV that were masked by larger peaks in the ^{61}V β-delayed γ-ray energy spectrum were found to be coincident with the 98-keV and 71-keV transitions, respectively, and placed in the ^{61}Cr level scheme based on the observed coincidences. The intensities of the 354- and 645-keV transitions listed in Table I were determined by scaling to other γ rays seen in both the β-delayed γ singles spectrum and γ-γ coincidence spectra. Only the 577-keV transition, with a relatively small absolute intensity of 0.7%, could not be placed in the ^{61}Cr level scheme. It is possible that the 577-keV transition depopulates the 1026-keV state and feeds the 451-keV state, but the statistics were not sufficient to confirm this assumption. The 71-keV transition is limited to having dipole character based on Weisskopf estimates and the nonobservation of a lifetime for the 71-keV state. From the intensity of coincident 127- and 98-keV γ rays, an internal-conversion coefficient of 0.17(13) was inferred for the 98-keV transition, albeit with a large relative uncertainty. As no time delay was observed between the 127- and 98-keV γ rays within the experimental detection limit of approximately 150 ns, Weisskopf estimates would suggest a dipole or mixed $M1$-$E2$ 98-keV transition.

Based on the observed γ-ray transitions, it could be suggested that the 71- and 98-keV transitions populate two different isomeric states in ^{61}Cr. Indeed, no mutual coincidence was observed between any transition coincident with the 98-keV γ ray and any transition coincident with the 71-keV γ ray. However, no further supporting evidence for a ^{61}Cr

TABLE II. Energies and absolute intensities per 100 β decays for the γ-ray transitions identified in ^{63}Cr following the β decay of ^{63}V.

E (keV)	Abs. inten. (%)	E (keV)	Abs. inten. (%)
83.1(6)	4(2)	414.0(6)[a]	4(2)
120.3(4)	15(3)		

[a]Transition not placed in ^{63}Cr level scheme.

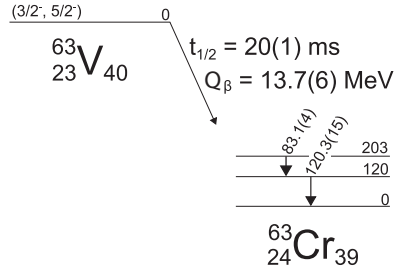

FIG. 7. Low-energy level scheme of ^{63}Cr inferred from the β decay of ^{63}V. The β-decay Q value was taken from Ref. [31] and was determined from systematics. The absolute intensity of each γ-ray transition is shown in parentheses following the transition energy.

isomer was found. An attempt was made to identify β-decaying isomeric states in ^{61}Cr by determining the time delay between selected β-delayed γ-ray transitions in ^{61}Cr and the subsequent β decay to ^{61}Mn. Within the uncertainty of the measurement, the β-decay half-life of ^{61}Cr following the 71-keV γ ray was the same as the ^{61}Cr half-life following the 98-keV γ ray, and both were consistent with the half-life extracted from the β-decay curve generated by gating on the independently produced ^{61}Cr ions in the particle identification plot. Additionally, a search for isomeric γ-ray decays in ^{61}Cr within a 10-ms time period following ^{61}V β decay was conducted but returned no evidence for an isomeric state.

The ^{61}Cr ground state was originally assigned as $5/2^-$ [24] and attributed to the $\nu[303]5/2^-$ state which, according to Nilsson diagrams, would be expected to be the lowest-energy state for modest prolate deformations [24,32]. The apparent β-decay feedings deduced in Ref. [27] for the decay of ^{61}Cr to ^{61}Mn were consistent with a $5/2^-$ ^{61}Cr ground state. The previously assigned $5/2^-$ spin and parity is retained for the ^{61}Cr ground state in Fig. 5. The ^{61}Cr level scheme is discussed further in Sec. IV.

Assuming the β-decay parent nucleus $^{61}_{23}V_{38}$ is also deformed, $3/2^-$ or $5/2^-$ is likely its ground-state spin and parity. In Ref. [24], the ^{61}V ground state was inferred to be $3/2^-$ based on the odd proton filling the [321]$3/2^-$ state originating from the $f_{7/2}$ orbital. Nilsson diagrams predict such a $3/2^-$ ground-state configuration over a large range of prolate deformations [32]. The possibility of oblate deformation in the neighboring odd-A V isotope $^{59}V_{36}$ has also been suggested [30]. If there is a systematic trend of oblate ground states that continues into ^{61}V, a $5/2^-$ ground state would be expected. The lack of significant population of the first excited 4^+ state in ^{60}Cr following $\beta - n$ decay from ^{61}V favors the $3/2^-$ assignment for the ^{61}V ground state. For either the $3/2^-$ or $5/2^-$ ground state, a large β-decay feeding to the ground state of ^{61}Cr might be expected. The upper limit for ground-state feeding based on the present data is 40%.

B. ^{63}Cr

The β-delayed γ-ray energy spectrum observed within 150 ms after the arrival of a ^{63}V ion is shown in Fig. 6(a). The three γ rays listed in Table II are assigned as transitions in ^{63}Cr and observed for the first time. As previously reported in Ref. [25], an intense peak is seen in the β-delayed γ-ray energy spectrum at 446 keV due to the $2^+ \rightarrow 0^+$ transition in ^{62}Cr, which occurs following β-delayed neutron emission

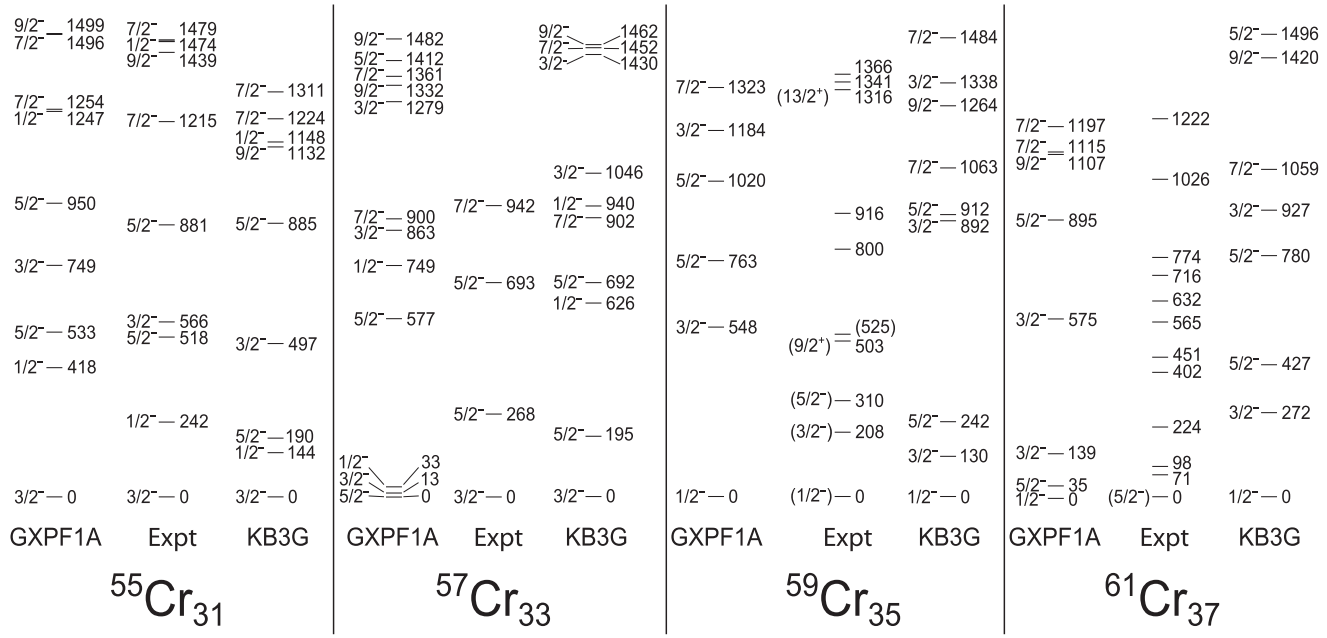

FIG. 8. Comparison of known experimental energy levels in ^{55,57,59,61}Cr with shell-model calculations. Experimental data for ^{55,57,59}Cr were taken from Refs. [38–41]. The levels reported at 828 and 1084 keV in ^{59}Cr in Ref. [41] are not displayed in the experimental level scheme for ^{59}Cr. Deep-inelastic-scattering data suggest that the 518-keV γ-ray transition [41] was incorrectly placed in the level scheme [42]. The energy of the 525-keV level in the experimental ^{59}Cr level scheme is shown in parentheses to indicate the tentative nature of its identification [40]. Although a γ-ray cascade was observed, the order of the 841- and 317-keV transitions could not be determined in Ref. [40]. If the order of the transitions is reversed compared to the tentative assignment, the level shown at 525 keV would instead be at 1042 keV.

TABLE III. Main neutron configurations of the $1/2_1^-$, $3/2_1^-$, and $5/2_1^-$ levels in ^{55,57,59,61}Cr as determined by the shell-model calculations. Configurations with a probability of 0.10 or greater are shown.

		GXPF1A		KB3G	
Isotope	J^π	Wave function (neutron)	Probability	Wave function (neutron)	Probability
^{55}Cr	$1/2_1^-$	$(0f_{7/2})^8,(1p_{3/2})^2,(0f_{5/2})^1,(1p_{1/2})^0$	0.24	$(0f_{7/2})^8,(1p_{3/2})^2,(0f_{5/2})^1,(1p_{1/2})^0$	0.26
		$(0f_{7/2})^8,(1p_{3/2})^2,(0f_{5/2})^0,(1p_{1/2})^1$	0.22	$(0f_{7/2})^8,(1p_{3/2})^1,(0f_{5/2})^1,(1p_{1/2})^1$	0.18
		$(0f_{7/2})^8,(1p_{3/2})^1,(0f_{5/2})^1,(1p_{1/2})^1$	0.16	$(0f_{7/2})^8,(1p_{3/2})^2,(0f_{5/2})^0,(1p_{1/2})^1$	0.14
	$3/2_1^-$	$(0f_{7/2})^8,(1p_{3/2})^3,(0f_{5/2})^0,(1p_{1/2})^0$	0.47	$(0f_{7/2})^8,(1p_{3/2})^3,(0f_{5/2})^0,(1p_{1/2})^0$	0.37
		$(0f_{7/2})^8,(1p_{3/2})^2,(0f_{5/2})^0,(1p_{1/2})^1$	0.11		
	$5/2_1^-$	$(0f_{7/2})^8,(1p_{3/2})^2,(0f_{5/2})^1,(1p_{1/2})^0$	0.44	$(0f_{7/2})^8,(1p_{3/2})^2,(0f_{5/2})^1,(1p_{1/2})^0$	0.42
		$(0f_{7/2})^8,(1p_{3/2})^1,(0f_{5/2})^1,(1p_{1/2})^1$	0.10		
^{57}Cr	$1/2_1^-$	$(0f_{7/2})^8,(1p_{3/2})^4,(0f_{5/2})^0,(1p_{1/2})^1$	0.51	$(0f_{7/2})^8,(1p_{3/2})^4,(0f_{5/2})^0,(1p_{1/2})^1$	0.19
		$(0f_{7/2})^8,(1p_{3/2})^2,(0f_{5/2})^2,(1p_{1/2})^1$	0.12	$(0f_{7/2})^8,(1p_{3/2})^4,(0f_{5/2})^1,(1p_{1/2})^0$	0.18
				$(0f_{7/2})^8,(1p_{3/2})^3,(0f_{5/2})^2,(1p_{1/2})^0$	0.14
				$(0f_{7/2})^8,(1p_{3/2})^3,(0f_{5/2})^1,(1p_{1/2})^1$	0.10
	$3/2_1^-$	$(0f_{7/2})^8,(1p_{3/2})^3,(0f_{5/2})^2,(1p_{1/2})^0$	0.39	$(0f_{7/2})^8,(1p_{3/2})^3,(0f_{5/2})^2,(1p_{1/2})^0$	0.47
		$(0f_{7/2})^8,(1p_{3/2})^3,(0f_{5/2})^1,(1p_{1/2})^1$	0.12		
	$5/2_1^-$	$(0f_{7/2})^8,(1p_{3/2})^4,(0f_{5/2})^1,(1p_{1/2})^0$	0.45	$(0f_{7/2})^8,(1p_{3/2})^4,(0f_{5/2})^1,(1p_{1/2})^0$	0.38
		$(0f_{7/2})^8,(1p_{3/2})^3,(0f_{5/2})^1,(1p_{1/2})^1$	0.15	$(0f_{7/2})^8,(1p_{3/2})^3,(0f_{5/2})^1,(1p_{1/2})^1$	0.15
				$(0f_{7/2})^8,(1p_{3/2})^2,(0f_{5/2})^1,(1p_{1/2})^2$	0.10
^{59}Cr	$1/2_1^-$	$(0f_{7/2})^8,(1p_{3/2})^4,(0f_{5/2})^2,(1p_{1/2})^1$	0.63	$(0f_{7/2})^8,(1p_{3/2})^4,(0f_{5/2})^2,(1p_{1/2})^1$	0.60
	$3/2_1^-$	$(0f_{7/2})^8,(1p_{3/2})^4,(0f_{5/2})^2,(1p_{1/2})^1$	0.44	$(0f_{7/2})^8,(1p_{3/2})^4,(0f_{5/2})^3,(1p_{1/2})^0$	0.36
		$(0f_{7/2})^8,(1p_{3/2})^4,(0f_{5/2})^3,(1p_{1/2})^0$	0.12	$(0f_{7/2})^8,(1p_{3/2})^4,(0f_{5/2})^2,(1p_{1/2})^1$	0.22
		$(0f_{7/2})^8,(1p_{3/2})^3,(0f_{5/2})^2,(1p_{1/2})^2$	0.11		
	$5/2_1^-$	$(0f_{7/2})^8,(1p_{3/2})^4,(0f_{5/2})^1,(1p_{1/2})^2$	0.28	$(0f_{7/2})^8,(1p_{3/2})^4,(0f_{5/2})^3,(1p_{1/2})^0$	0.47
		$(0f_{7/2})^8,(1p_{3/2})^4,(0f_{5/2})^3,(1p_{1/2})^0$	0.21	$(0f_{7/2})^8,(1p_{3/2})^3,(0f_{5/2})^3,(1p_{1/2})^1$	0.11
		$(0f_{7/2})^8,(1p_{3/2})^4,(0f_{5/2})^2,(1p_{1/2})^1$	0.15	$(0f_{7/2})^8,(1p_{3/2})^2,(0f_{5/2})^3,(1p_{1/2})^2$	0.10
^{61}Cr	$1/2_1^-$	$(0f_{7/2})^8,(1p_{3/2})^4,(0f_{5/2})^4,(1p_{1/2})^1$	0.76	$(0f_{7/2})^8,(1p_{3/2})^4,(0f_{5/2})^4,(1p_{1/2})^1$	0.75
	$3/2_1^-$	$(0f_{7/2})^8,(1p_{3/2})^4,(0f_{5/2})^3,(1p_{1/2})^2$	0.71	$(0f_{7/2})^8,(1p_{3/2})^4,(0f_{5/2})^4,(1p_{1/2})^1$	0.44
		$(0f_{7/2})^8,(1p_{3/2})^4,(0f_{5/2})^4,(1p_{1/2})^1$	0.13	$(0f_{7/2})^8,(1p_{3/2})^4,(0f_{5/2})^3,(1p_{1/2})^2$	0.33
	$5/2_1^-$	$(0f_{7/2})^8,(1p_{3/2})^4,(0f_{5/2})^3,(1p_{1/2})^2$	0.78	$(0f_{7/2})^8,(1p_{3/2})^4,(0f_{5/2})^3,(1p_{1/2})^2$	0.60
				$(0f_{7/2})^8,(1p_{3/2})^4,(0f_{5/2})^4,(1p_{1/2})^1$	0.10

from ^{63}V. The $\beta - n$ branching ratio is found to be at least 29% in the present experiment. No population of the 4_1^+ state in ^{62}Cr was observed following $\beta - n$ decay from ^{63}V. The maximum branching ratio to the 4_1^+ state in ^{62}Cr is inferred to be 4%.

The ^{63}V β-decay curve is shown in Fig. 6(b). It was fit considering contributions from the decay of ^{63}V, ^{63}Cr (129 ms [24]), ^{63}Mn (275 ms [4]), ^{62}Cr (209 ms [24]), and ^{62}Mn (92 ms [24]) and a constant background, where the values in parentheses refer to half-lives that were fixed according to literature values. The fraction of decays due to $\beta - n$ emission was fixed based on the absolute intensity of the 446-keV γ-ray transition. The half-life of ^{63}V was found to be 20(1) ms, in agreement with previous results of 17(3) ms [25] and 19.2(24) ms [15]. Like the fit for ^{61}V, the intensity of the $\beta - n$ branch had a small impact on the extracted ^{63}V half-life. Varying the branching ratio by a factor of 2 changed the half-life by less than 1 ms.

The low-energy scheme for ^{63}Cr following the β decay of ^{63}V is shown in Fig. 7. The 83- and 120-keV γ rays are coincident, as indicated by the inset of Fig. 6(a). Based on the absolute intensities of the 83- and 120-keV transitions, the 83-keV γ ray is proposed to feed a 120-keV state. If the 83-keV transition is highly converted, it is also possible that the ordering of the 83- and 120-keV transitions is reversed and the 120-keV γ ray feeds an 83-keV state. The 83- and 120-keV transitions are most likely of dipole character, or perhaps are collective $E2$ transitions, based on Weisskopf estimates and the lack of observed lifetimes for the 203- and 120-keV states. The 414-keV transition, which had an absolute intensity of 4(2)%, could not be placed in the ^{63}Cr level scheme.

Based on systematics, the ground state of ^{63}V is expected to be $3/2^-$ or $5/2^-$. The nonobservation of the population of the first excited 4^+ state in ^{62}Cr following β-delayed neutron emission from ^{63}V favors the $3/2^-$ spin and parity of the ^{63}V ground state. A spin and parity of $3/2^-$ would be consistent with ascribing the ground state to the $[321]3/2^-$ state for a prolate-deformed ^{63}V.

The low-energy structure of ^{63}Cr is dramatically different from isotonic ^{65}Fe. Namely, a gap of over 350 keV between the ground and first excited states in ^{65}Fe [14,33] does not exist in ^{63}Cr. Further, while two long-lived isomers with half-lives of hundreds of nanoseconds or longer are known in ^{65}Fe around 400 keV [14,33,34], none have been discovered in ^{63}Cr.

IV. DISCUSSION

Shell-model calculations were carried out to further understand the low-energy level schemes of the neutron-rich

odd-A Cr isotopes. The calculations were performed using the GXPF1A [35] and KB3G [36] effective interactions in the fp shell with NUSHELLX [37]. The calculated and known experimental energy levels below 1.5 MeV in ^{55,57,59,61}Cr are compared in Fig. 8.

The lowest-energy states calculated by the GXPF1A and KB3G interactions can be interpreted rather straightforwardly. The calculations using the two different effective interactions predict that the three lowest-energy states in ^{55,57,59,61}Cr have, in some order, spins and parities of $1/2^-$, $3/2^-$, and $5/2^-$. The most important neutron configurations contributing to the $1/2_1{}^-$, $3/2_1{}^-$, and $5/2_1{}^-$ states calculated with the GXPF1A and KB3G interactions are given in Table III. The calculations predict that the $5/2_1{}^-$ state is dominated by an odd neutron occupying the $f_{5/2}$ orbital in all four of the odd-A Cr isotopes. In ^{55}Cr, an odd neutron occupying the $p_{1/2}$ orbital is an important configuration of the $1/2_1{}^-$ state, but other configurations also contribute significantly. While the GXPF1A and KB3G interactions predict somewhat varying probabilities of the $(0f_{7/2})^8$,$(1p_{3/2})^4$,$(0f_{5/2})^0$,$(1p_{1/2})^1$ configuration in the $1/2_1{}^-$ state in ^{57}Cr, both clearly calculate configurations with one neutron in the $1p_{1/2}$ orbital to be the dominant neutron configuration in the $1/2_1{}^-$ states in ^{59,61}Cr. The $3/2_1{}^-$ states in ^{55,57}Cr are predicted to be primarily described by configurations with three neutrons in the $p_{3/2}$ orbital. However, by ^{59}Cr the $p_{3/2}$ orbital is completely occupied, and the odd neutrons are distributed among the $f_{5/2}$ and $p_{1/2}$ single-particle states.

In ^{55}Cr there is a one-to-one correspondence between the experimentally measured energy levels and the calculated states below 1.5 MeV. The comparison of the calculations with experiment is adequate for ^{57}Cr, but the calculations suggest some states have not yet been observed experimentally. ^{59}Cr is a transitional nucleus. The agreement between theory and experiment is still reasonable at low energies for the negative-parity states. However, the calculations within the fp shell cannot account for the experimentally observed $(9/2^+)$ state, which originates from the $g_{9/2}$ orbital outside of the model space. In ^{61}Cr, there are far more experimentally observed energy levels below 800 keV than can be accounted for with the GXPF1A or KB3G interactions. Although the calculations predict that the low-energy level scheme of ^{61}Cr should be quite similar to the three previous lighter odd-A Cr isotopes, this is not the case. The likely cause is the onset of deformation caused by the influence of the $\nu g_{9/2}$ intruder orbital. Indeed, the excitation of the $9/2_1{}^+$ state has been observed to rapidly decrease in the odd-A Cr isotopes, dropping from 3707 keV in ^{53}Cr [43] to 503 keV in ^{59}Cr [33]. Given the increased low-energy level density in ^{61}Cr relative to the lighter odd-A Cr isotopes, it is probable that both positive- and negative-parity states have been observed in the present experiment. The dramatic increase in level density could also explain the absence of a low-energy isomeric state in both ^{61,63}Cr, in contrast to most other $N = 37$ and $N = 39$ isotones from Ti to Ni [30,33,34,44–50].

V. CONCLUSION

The nuclei ^{61,63}Cr were populated by the β decay of ^{61,63}V. Thirteen excited states have been identified in ^{61}Cr, greatly extending the previously proposed level scheme [24]. A stark contrast was observed between the low-energy level schemes of ^{61}Cr and the neighboring lighter odd-A Cr isotopes. In particular, a high level density was observed in ^{61}Cr, and the presence of low-energy positive-parity states is inferred based on the influence of the $\nu g_{9/2}$ orbital. The increased low-energy level density could also explain the lack of isomers in ^{61,63}Cr. Additionally, γ-ray transitions were observed in ^{63}Cr for the first time.

ACKNOWLEDGMENTS

This work was funded in part by the NSF under Contract No. PHY-1102511 (NSCL) and the DOE under Contracts No. DE-NA0000979 (NNSA) and No. DE-AC02-06CH11357 (ANL), and Grant No. DE-FG02-94-ER40834 (UM).

[1] R. Broda, B. Fornal, W. Królas, T. Pawłat, D. Bazzacco, S. Lunardi, C. Rossi-Alvarez, R. Menegazzo, G. de Angelis, P. Bednarczyk, J. Rico, D. De Acuña, P. J. Daly, R. H. Mayer, M. Sferrazza, H. Grawe, K. H. Maier, and R. Schubart, Phys. Rev. Lett. **74**, 868 (1995).

[2] F. Azaiez, Phy. Scr. **T88**, 118 (2000).

[3] O. Sorlin *et al.*, Phys. Rev. Lett. **88**, 092501 (2002).

[4] M. Hannawald, T. Kautzsch, A. Wöhr, W. B. Walters, K.-L. Kratz, V. N. Fedoseyev, V. I. Mishin, W. Böhmer, B. Pfeiffer, V. Sebastian, Y. Jading, U. Köster, J. Lettry, H. L. Ravn, and the ISOLDE Collaboration, Phys. Rev. Lett. **82**, 1391 (1999).

[5] A. Gade, R. V. F. Janssens, T. Baugher, D. Bazin, B. A. Brown, M. P. Carpenter, C. J. Chiara, A. N. Deacon, S. J. Freeman, G. F. Grinyer, C. R. Hoffman, B. P. Kay, F. G. Kondev, T. Lauritsen, S. McDaniel, K. Meierbachtol, A. Ratkiewicz, S. R. Stroberg, K. A. Walsh, D. Weisshaar, R. Winkler, and S. Zhu, Phys. Rev. C **81**, 051304(R) (2010).

[6] W. Rother, A. Dewald, H. Iwasaki, S. M. Lenzi, K. Starosta, D. Bazin, T. Baugher, B. A. Brown, H. L. Crawford, C. Fransen, A. Gade, T. N. Ginter, T. Glasmacher, G. F. Grinyer, M. Hackstein, G. Ilie, J. Jolie, S. McDaniel, D. Miller, P. Petkov, T. Pissulla, A. Ratkiewicz, C. A. Ur, P. Voss, K. A. Walsh, D. Weisshaar, and K.-O. Zell, Phys. Rev. Lett. **106**, 022502 (2011).

[7] T. Baugher, A. Gade, R. V. F. Janssens, S. M. Lenzi, D. Bazin, B. A. Brown, M. P. Carpenter, A. N. Deacon, S. J. Freeman, T. Glasmacher, G. F. Grinyer, F. G. Kondev, S. McDaniel, A. Poves, A. Ratkiewicz, E. A. McCutchan, D. K. Sharp, I. Stefanescu, K. A. Walsh, D. Weisshaar, and S. Zhu, Phys. Rev. C **86**, 011305(R) (2012).

[8] H. L. Crawford, R. M. Clark, P. Fallon, A. O. Macchiavelli, T. Baugher, D. Bazin, C. W. Beausang, J. S. Berryman, D. L. Bleuel, C. M. Campbell, M. Cromaz, G. de Angelis, A. Gade, R. O. Hughes, I. Y. Lee, S. M. Lenzi, F. Nowacki, S. Paschalis, M. Petri, A. Poves, A. Ratkiewicz, T. J. Ross, E. Sahin,

D. Weisshaar, K. Wimmer, and R. Winkler, Phys. Rev. Lett. **110**, 242701 (2013).
[9] E. Caurier, F. Nowacki, and A. Poves, Eur. Phys. J. A **15**, 145 (2002).
[10] S. M. Lenzi, F. Nowacki, A. Poves, and K. Sieja, Phys. Rev. C **82**, 054301 (2010).
[11] D. Pauwels, O. Ivanov, N. Bree, J. Büscher, T. E. Cocolios, J. Gentens, M. Huyse, A. Korgul, Y. Kudryavtsev, R. Raabe, M. Sawicka, I. Stefanescu, J. Van de Walle, P. Van den Bergh, P. Van Duppen, and W. B. Walters, Phys. Rev. C **78**, 041307(R) (2008).
[12] D. Pauwels *et al*., Phys. Rev. C **79**, 044309 (2009).
[13] E. K. Warburton, J. W. Olness, A. M. Nathan, J. J. Kolata, and J. B. McGrory, Phys. Rev. C **16**, 1027 (1977).
[14] B. Olaizola, L. M. Fraile, H. Mach, A. Aprahamian, J. A. Briz, J. Cal-González, D. Ghiţa, U. Köster, W. Kurcewicz, S. R. Lesher, D. Pauwels, E. Picado, A. Poves, D. Radulov, G. S. Simpson, and J. M. Udías, Phys. Rev. C **88**, 044306 (2013).
[15] J. M. Daugas *et al*., Phys. Rev. C **83**, 054312 (2011).
[16] S. N. Liddick, S. Suchyta, B. Abromeit, A. Ayres, A. Bey, C. R. Bingham, M. Bolla, M. P. Carpenter, L. Cartegni, C. J. Chiara, H. L. Crawford, I. G. Darby, R. Grzywacz, G. Gürdal, S. Ilyushkin, N. Larson, M. Madurga, E. A. McCutchan, D. Miller, S. Padgett, S. V. Paulauskas, J. Pereira, M. M. Rajabali, K. Rykaczewski, S. Vinnikova, W. B. Walters, and S. Zhu, Phys. Rev. C **84**, 061305 (2011).
[17] S. N. Liddick, B. Abromeit, A. Ayres, A. Bey, C. R. Bingham, M. Bolla, L. Cartegni, H. L. Crawford, I. G. Darby, R. Grzywacz, S. Ilyushkin, N. Larson, M. Madurga, D. Miller, S. Padgett, S. Paulauskas, M. M. Rajabali, K. Rykaczewski, and S. Suchyta, Phys. Rev. C **85**, 014328 (2012).
[18] C. J. Chiara, I. Stefanescu, N. Hoteling, W. B. Walters, R. V. F. Janssens, R. Broda, M. P. Carpenter, B. Fornal, A. A. Hecht, W. Królas, T. Lauritsen, T. Pawłat, D. Seweryniak, X. Wang, A. Wöhr, J. Wrzesiński, and S. Zhu, Phys. Rev. C **82**, 054313 (2010).
[19] D. J. Morrissey, B. M. Sherrill, M. Steiner, A. Stolz, and I. Wiedenhoever, Nucl. Instrum. Methods Phys. Res. B **204**, 90 (2003).
[20] J. I. Prisciandaro, A. C. Morton, and P. F. Mantica, Nucl. Instrum. Methods Phys. Res. A **505**, 140 (2003).
[21] W. F. Mueller, J. A. Church, T. Glasmacher, D. Gutknecht, G. Hackman, P. G. Hansen, Z. Hu, K. L. Miller, and P. Quirin, Nucl. Instrum. Methods Phys. Res. A **466**, 492 (2001).
[22] K. Starosta, C. Vaman, D. Miller, P. Voss, D. Bazin, T. Glasmacher, H. Crawford, P. Mantica, H. Tan, W. Hennig, M. Walby, A. Fallu-Labruyere, J. Harris, D. Breus, P. Grudberg, and W. K. Warburton, Nucl. Instrum. Methods Phys. Res. A **610**, 700 (2009).
[23] C. J. Prokop, S. N. Liddick, B. L. Abromeit, A. T. Chemey, N. R. Larson, S. Suchyta, and J. R. Tompkins, Nucl. Instrum. Methods Phys. Res. A **741**, 163 (2014).
[24] L. Gaudefroy, O. Sorlin, C. Donzaud, J. C. Angélique, F. Azaiez, C. Bourgeois, V. Chiste, Z. Dlouhy, S. Grévy, D. Guillemaud-Mueller, F. Ibrahim, K.-L. Kratz, M. Lewitowicz, S. M. Lukyanov, I. Matea, J. Mrasek, F. Nowacki, F. de Oliveira Santos, Y.-E. Penionzhkevich, B. Pfeiffer, F. Pougheon, M. G. Saint-Laurent, and M. Stanoiu, Eur. Phys. J. A **23**, 41 (2005).
[25] O. Sorlin, C. Donzaud, F. Nowacki, J. C. Angélique, F. Azaiez, C. Bourgeois, V. Chiste, Z. Dlouhy, S. Grévy, D. Guillemaud-Mueller, F. Ibrahim, K.-L. Kratz, M. Lewitowicz, S. M. Lukyanov, J. Mrasek, Y.-E. Penionzhkevich, F. de Oliveira Santos, B. Pfeiffer, F. Pougheon, A. Poves, M. G. Saint-Laurent, and M. Stanoiu, Eur. Phys. J. A **16**, 55 (2003).
[26] S. Zhu, A. N. Deacon, S. J. Freeman, R. V. F. Janssens, B. Fornal, M. Honma, F. R. Xu, R. Broda, I. R. Calderin, M. P. Carpenter, P. Chowdhury, F. G. Kondev, W. Królas, T. Lauritsen, S. N. Liddick, C. J. Lister, P. F. Mantica, T. Pawłat, D. Seweryniak, J. F. Smith, S. L. Tabor, B. E. Tomlin, B. J. Varley, and J. Wrzesiński, Phys. Rev. C **74**, 064315 (2006).
[27] H. L. Crawford, P. F. Mantica, J. S. Berryman, R. Broda, B. Fornal, C. R. Hoffman, N. Hoteling, R. V. F. Janssens, S. M. Lenzi, J. Pereira, J. B. Stoker, S. L. Tabor, W. B. Walters, X. Wang, and S. Zhu, Phys. Rev. C **79**, 054320 (2009).
[28] M. R. Bhat, Nucl. Data Sheets **88**, 417 (1999).
[29] S. N. Liddick, P. F. Mantica, B. A. Brown, M. P. Carpenter, A. D. Davies, M. Horoi, R. V. F. Janssens, A. C. Morton, W. F. Mueller, J. Pavan, H. Schatz, A. Stolz, S. L. Tabor, B. E. Tomlin, and M. Wiedeking, Phys. Rev. C **73**, 044322 (2006).
[30] O. Sorlin, C. Donzaud, L. Axelsson, M. Belleguic, R. Béraud, C. Borcea, G. Canchel, E. Chabanat, J. M. Daugas, A. Emsallem, M. Girod, D. Guillemaud-Mueller, K.-L. Kratz, S. Leenhardt, M. Lewitowicz, C. Longour, M. J. Lopez, F. de Oliveira Santos, L. Petizon, B. Pfeiffer, F. Pougheon, M. G. Saint-Laurent, and J. E. Sauvestre, Nucl. Phys. A **669**, 351 (2000).
[31] M. Wang, G. Audi, A. H. Wapstra, F. G. Kondev, M. MacCormick, X. Xu, and B. Pfeiffer, Chin. Phys. C **36**, 1603 (2012).
[32] O. Sorlin, V. Borrel, S. Grévy, D. Guillemaud-Mueller, A. C. Mueller, F. Pougheon, W. Böhmer, K.-L. Kratz, T. Mehren, P. Möller, B. Pfeiffer, T. Rauscher, M. G. Saint-Laurent, R. Anne, M. Lewitowicz, A. Ostrowski, T. Dörfler, and W.-D. Schmidt-Ott, Nucl. Phys. A **632**, 205 (1998).
[33] R. Grzywacz, R. Béraud, C. Borcea, A. Emsallem, M. Glogowski, H. Grawe, D. Guillemaud-Mueller, M. Hjorth-Jensen, M. Houry, M. Lewitowicz, A. C. Mueller, A. Nowak, A. Płochocki, M. Pfützner, K. Rykaczewski, M. G. Saint-Laurent, J. E. Sauvestre, M. Schaefer, O. Sorlin, J. Szerypo, W. Trinder, S. Viteritti, and J. Winfield, Phys. Rev. Lett. **81**, 766 (1998).
[34] M. Block, C. Bachelet, G. Bollen, M. Facina, C. M. Folden, III, C. Guénaut, A. A. Kwiatkowski, D. J. Morrissey, G. K. Pang, A. Prinke, R. Ringle, J. Savory, P. Schury, and S. Schwarz, Phys. Rev. Lett. **100**, 132501 (2008).
[35] M. Honma, T. Otsuka, B. Brown, and T. Mizusaki, Eur. Phys. J. A **25**, 499 (2005).
[36] A. Poves, J. Sánchez-Solano, E. Caurier, and F. Nowacki, Nucl. Phys. A **694**, 157 (2001).
[37] B. A. Brown and W. D. M. Rae, http://www.nscl.msu.edu/~brown/resources/resources.html.
[38] H. Junde, Nucl. Data Sheets **109**, 787 (2008).
[39] A. N. Deacon, S. J. Freeman, R. V. F. Janssens, F. R. Xu, M. P. Carpenter, I. R. Calderin, P. Chowdhury, N. J. Hammond, T. Lauritsen, C. J. Lister, D. Seweryniak, J. F. Smith, S. L. Tabor, B. J. Varley, and S. Zhu, Phys. Lett. B **622**, 151 (2005).
[40] S. N. Liddick, P. F. Mantica, R. Broda, B. A. Brown, M. P. Carpenter, A. D. Davies, B. Fornal, M. Horoi, R. V. F. Janssens, A. C. Morton, W. F. Mueller, J. Pavan, H. Schatz, A. Stolz, S. L. Tabor, B. E. Tomlin, and M. Wiedeking, Phys. Rev. C **72**, 054321 (2005).
[41] S. J. Freeman, R. V. F. Janssens, B. A. Brown, M. P. Carpenter, S. M. Fischer, N. J. Hammond, M. Honma, T. Lauritsen, C. J.

Lister, T. L. Khoo, G. Mukherjee, D. Seweryniak, J. F. Smith, B. J. Varley, M. Whitehead, and S. Zhu, Phys. Rev. C **69**, 064301 (2004).
[42] J. Harker (private communication).
[43] H. Junde, Nucl. Data Sheets **110**, 2689 (2009).
[44] O. Sorlin, C. Donzaud, F. Azaiez, C. Bourgeois, L. Gaudefroy, F. Ibrahim, D. Guillemaud-Mueller, F. Pougheon, M. Lewitowicz, F. de Oliveira Santos, M. G. Saint-Laurent, M. Stanoiu, S. M. Lukyanov, Yu. E. Penionzhkevich, J. C. Angélique, S. Grévy, K.-L. Kratz, B. Pfeiffer, F. Nowacki, Z. Dlouhy, and J. Mrasek, Nucl. Phys. A **719**, C193 (2003).
[45] I. Matea, Ph.D. thesis, Universite de Caen/Basse-Normandie, 2002.
[46] J. M. Daugas, Ph.D. thesis, Universite de Caen/Basse-Normandie, 1999.
[47] S. Lunardi *et al.*, Phys. Rev. C **76**, 034303 (2007).
[48] J. M. Daugas *et al.*, Phys. Rev. C **81**, 034304 (2010).
[49] M. J. Murphy, C. N. Davids, E. B. Norman, and R. C. Pardo, Phys. Rev. C **17**, 1574 (1978).
[50] T. Pawłat, R. Broda, W. Królas, A. Maj, M. Zięblíński, H. Grawe, R. Schubart, K. H. Maier, J. Heese, H. Kluge, and M. Schramm, Nucl. Phys. A **574**, 623 (1994).